

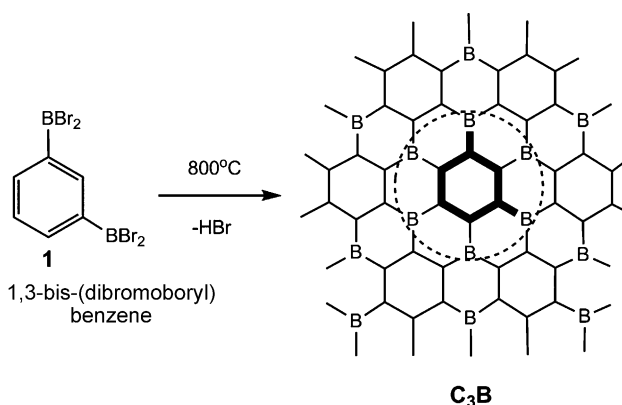
Theory and Practice: Bulk Synthesis of  $C_3B$  and its  $H_2$ - and Li-Storage Capacity\*\*

Timothy C. King, Peter D. Matthews, Hugh Glass, Jonathan A. Cormack, Juan Pedro Holgado, Michal Leskes, John M. Griffin, Oren A. Scherman, Paul D. Barker, Clare P. Grey, Siân E. Dutton, Richard M. Lambert, Gary Tustin, Ali Alavi,\* and Dominic S. Wright\*

In memory of Kenneth Wade

**Abstract:** Previous theoretical studies of  $C_3B$  have suggested that boron-doped graphite is a promising  $H_2$ - and Li-storage material, with large maximum capacities. These characteristics could lead to exciting applications as a lightweight  $H_2$ -storage material for automotive engines and as an anode in a new generation of batteries. However, for these applications to be realized a synthetic route to bulk  $C_3B$  must be developed. Here we show the thermolysis of a single-source precursor (1,3- $(BBr_2)_2C_6H_4$ ) to produce graphitic  $C_3B$ , thus allowing the characteristics of this elusive material to be tested for the first time.  $C_3B$  was found to be compositionally uniform but turbostratically disordered. Contrary to theoretical expectations, the  $H_2$ - and Li-storage capacities are lower than anticipated, results that can partially be explained by the disordered nature of the material. This work suggests that to model the properties of graphitic materials more realistically, the possibility of disorder must be considered.

The development of practical and efficient chemical and electrical power storage systems is particularly important with regard to mobile applications such as sustainable automotive transport and consumer electronics.<sup>[1–3]</sup> Safe and recyclable  $H_2$ -<sup>[4]</sup> and Li-storage<sup>[5]</sup> systems which have high energy-to-weight ratios are at the cutting edge of materials and engineering design. The boron carbide  $C_3B$  (Scheme 1) has been of great interest to materials scientists and physicists since it was first reported over a quarter of a century ago,<sup>[6]</sup> owing to the presence of electron-poor, substitutional boron in the parent lattice of graphite, which results in increased



**Scheme 1.** The synthetic route to the formation of idealized  $C_3B$ . The structure shown here is that proposed by Bartlett and co-workers.<sup>[6]</sup>

conductivity.<sup>[7]</sup> A recent resurgence of interest in this material has resulted from theoretical evidence that bulk samples of  $C_3B$  may be a viable, high-capacity  $H_2$ -storage material at moderate temperatures and pressures<sup>[8,9]</sup> (up to 6.1 wt %, over the US Department of Energy storage target).<sup>[10]</sup> In addition, calculations have shown that  $C_3B$  may have a Li capacity of  $857 \text{ mA h g}^{-1}$ , over twice that of graphite, the anode material commercially used in batteries ( $372 \text{ mA h g}^{-1}$ ).<sup>[11,12]</sup> Crucially, however, the projected  $H_2$ -storage properties of  $C_3B$  are reliant on the presence of multilayered, bulk samples. Calculations reveal that the most likely mechanism of  $H_2$  absorption involves chemisorption of  $H_2$  progressing by

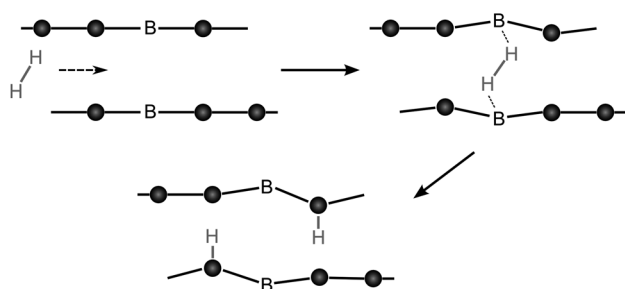
[\*] T. C. King, P. D. Matthews, H. Glass, J. A. Cormack, Dr. M. Leskes, Dr. J. M. Griffin, Dr. P. D. Barker, Prof. C. P. Grey, Prof. A. Alavi, Prof. D. S. Wright  
Department of Chemistry, University of Cambridge  
Lensfield Road, Cambridge, CB2 1EW (UK)  
E-mail: asa10@cam.ac.uk  
dsw1000@cam.ac.uk

Dr. J. P. Holgado, Prof. R. M. Lambert  
Instituto de Ciencia de Materiales de Sevilla, CSIC-Univ. Sevilla  
Av. Americo Vespucio 49, 41092 Sevilla (Spain)  
Dr. O. A. Scherman  
Melville Laboratory for Polymer Synthesis, University of Cambridge  
Lensfield Road, Cambridge, CB2 1EW (UK)  
Dr. S. E. Dutton  
Cavendish Laboratory, University of Cambridge  
JJ Thomson Ave., Cambridge, CB3 0HE (UK)

Dr. G. Tustin  
Schlumberger Gould Research Centre  
High Cross, Madingley Road, Cambridge, CB3 0EL (UK)  
Prof. A. Alavi  
Max Planck Institute for Solid state Research  
Heisenbergstrasse 1, Stuttgart 70569, Germany.

[\*\*] We thank the ERC (Advance Investigator awards for D.S.W., C.P.G.), the EPSRC (T.C.K., P.D.M., H.G., J.C.), and the Spanish Ministerio de Economía y Competitividad (under grants ENE2011-24-412 and IPT-2011-1553-420000). We thank John Bulmer for Raman spectroscopy and Keith Parmenter for glass blowing. We thank the Schlumberger Gould Research Centre for XPS analysis.

Supporting information for this article is available on the WWW under <http://dx.doi.org/10.1002/anie.201412200>.



**Scheme 2.** Process of  $\text{H}_2$  intercalation followed by boron-assisted activation and C–H bond formation. Black spheres represent carbon.

homolytic, boron-assisted cleavage of the H–H bonds with the ultimate formation of two C–H bonds (Scheme 2) with a low kinetic barrier for the initial  $\text{H}_2$  intercalation. Significantly, because the pathway involves interlayer activation of  $\text{H}_2$  molecules, pure graphite and discrete  $\text{C}_3\text{B}$  monolayers are predicted to show no hydrogen sorption.<sup>[8]</sup> In addition, the theoretical Li capacity of bulk  $\text{C}_3\text{B}$  (as  $\text{C}_3\text{BLi}_{1.5}$ ) is predicted to be higher than that of the monolayer.<sup>[12]</sup>

To date only microgram quantities of bulk  $\text{C}_3\text{B}$  have ever been prepared because of the inherent slowness and poor scalability of the existing chemical method used for its preparation: chemical vapor deposition (CVD) of  $\text{BCl}_3$  and  $\text{C}_6\text{H}_6$ .<sup>[13,14]</sup> While a standard chemical route involving the Wurtz coupling reaction of hexachlorobenzene ( $\text{C}_6\text{Cl}_6$ ) or tetrachloroethylene ( $\text{Cl}_2\text{C}=\text{CCl}_2$ ) and  $\text{BCl}_3$  with sodium metal in high boiling-point solvents has been used to produce boron-enriched graphite on the gram scale, the level of boron inclusion in this material (ca. 7.3 at. %) falls well short of that found in  $\text{C}_3\text{B}$  (25 at. %); in addition, high levels of oxidized species are present in the material.<sup>[15]</sup> It should be noted that the maximum boron content that can be obtained because of the solubility of boron in graphite is a mere 2.3%, and requires temperatures in excess of 2300 °C.<sup>[16]</sup>

We show here that the thermolysis of the simple aromatic boron compound 1,3-bis(dibromoboryl)benzene ( $1,3\text{-}(\text{BBr}_2)_2\text{C}_6\text{H}_4$ , **1**; Scheme 1),<sup>[17]</sup> which contains the correct 3:1 C/B stoichiometry, produces bulk samples of  $\text{C}_3\text{B}$  quantitatively, a reaction that can be scaled up to the gram scale. This “tiling” synthetic approach is a strategy which has previously shown potential in the synthesis of nitrogen-doped graphitic systems,<sup>[18]</sup> but is the first known single-source approach to  $\text{C}_3\text{B}$ . This has enabled the first experimental studies of the  $\text{H}_2$ - and Li-storage capacity of  $\text{C}_3\text{B}$  and a fundamentally important test of theory.

A previous report on the carbonization of *o*-phenylenediamine ( $1,2\text{-}(\text{NH}_2)_2\text{C}_6\text{H}_4$ ) at 800 °C to produce the related graphitic material ( $\text{C}_3\text{N}$ ) had shown the formation of two distinct materials, flakes and multiwalled graphite microspheres.<sup>[18]</sup> The formation of similar graphite microspheres was noted in our initial investigations on the thermolysis of **1** under these conditions (see Section S3 in the Supporting Information). However, optimization of the heating profile enabled the selective synthesis of  $\text{C}_3\text{B}$  flakes. The surface morphology of flakes of  $\text{C}_3\text{B}$  is seen in Figure 1 a, which shows a scanning electron microscopy (SEM) image of flakes which

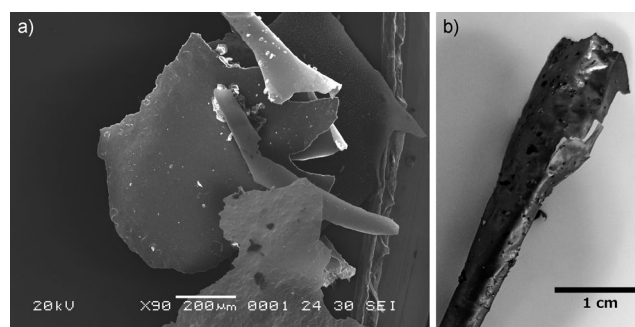


**Figure 1.** a) SEM image of  $\text{C}_3\text{B}$  typical flakes. b) Photograph of the  $\text{C}_3\text{B}$  material.

have typical thicknesses of 1 to 3  $\mu\text{m}$  and homogeneous sample make-up (see Section S4 in the Supporting Information). Macroscopically, these flakes of  $\text{C}_3\text{B}$  have a metallic luster (Figure 1 b). The curling of the flakes has been put down to their formation through the deposition of graphitic material onto the inside walls of a curved reaction vessel, thereby leading to a curl when the flakes detach from the walls.

The material was further characterized using Raman spectroscopy, powder X-ray diffraction (pXRD), X-ray photoelectron spectroscopy (XPS), solid-state  $^{11}\text{B}$  NMR spectroscopy, and laser-desorption/ionization time of flight mass spectrometry (LDI-TOF MS). These techniques show that boron substitution of the samples of  $\text{C}_3\text{B}$  is compositionally uniform within the bulk but that the graphitic structure is turbostratically disordered.

The graphitic nature of the material was shown by pXRD and Raman spectroscopy. The pXRD pattern (Figure 2) shows two main, broad reflections at  $\theta = 26^\circ$  (002) and  $43^\circ$

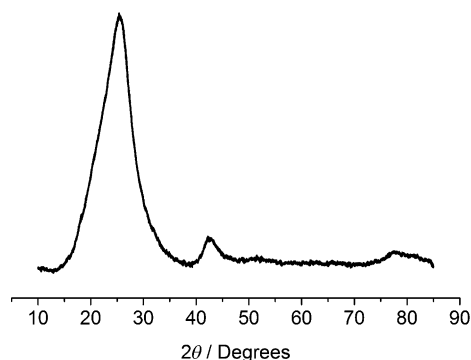


**Figure 2.** XRD of  $\text{C}_3\text{B}$  flakes. The broad peaks at  $26^\circ$ ,  $42^\circ$ , and  $78^\circ$  correspond to the (002), (100), and (110) planes of graphite.

(100), as well as a weaker reflection at  $78^\circ$  (110), thus indicating that the interlayer spacing and mean C–C/C–B bond length in  $\text{C}_3\text{B}$  are similar to the corresponding parameters in graphite. The broadness of the peaks is attributed to the turbostratic nature of the material, in which the layers do not exhibit periodic ordering with respect to one another; the asymmetry of the (002) reflection is ascribed to fluctuations in the interlayer spacing due to curvature in  $\text{C}_3\text{B}$  sheets as

prepared. The presence of disorder is consistent with previous DFT calculations on the packing of  $C_3B$ , which indicate that the different packing alternatives of the layers have very similar energies (no more than  $2.1 \text{ kJ mol}^{-1}$  between them).<sup>[19,20]</sup> Figure 3 shows the Raman spectrum of  $C_3B$  and

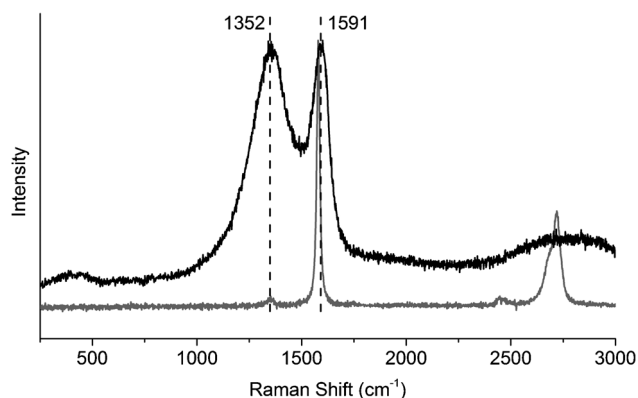


**Figure 3.** Raman spectrum of  $C_3B$  (black) and graphite (gray). The D, G, and 2D bands are seen at 1352, 1591, and 2720  $\text{cm}^{-1}$ , respectively

a sample of pristine graphite for comparison. The decrease in the  $I_{2D}/I_G$  ratio and increase in intensity of the D band (i.e. an increased  $I_D/I_G$  ratio) are both consistent with high dopant levels as well as the turbostratic nature of the sample.

Compositional analysis was performed using XPS. As XPS is a surface analysis technique, Ar ion beam etching was utilized to enable analysis through the depth of the material. Figure 4 shows how the elemental composition changes with

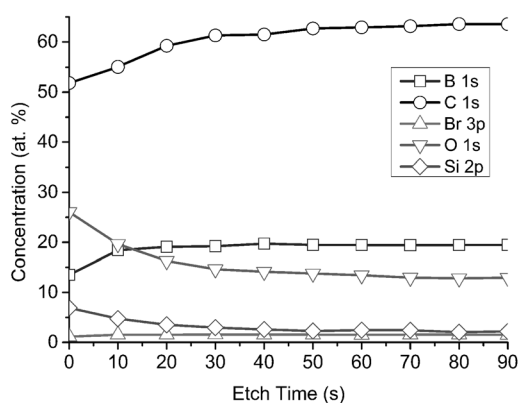


**Figure 4.** Elemental composition of  $C_3B$  flakes as a function of depth (achieved by increasing Ar ion etch time) determined by XPS analysis.

depth. The presence of Si can be attributed to the surface contamination with silica, resulting from the quartz tubes used in the synthesis. Consistent with this conclusion, the levels of Si and O fall off sharply with increased depth. XPS analysis of samples treated with HF show that this contamination is completely removed. The apparently consistently high level of oxygen present in samples, even at depth, is attributed to adventitious (background) contamination (see

the Supporting Information for further discussion).<sup>[21]</sup> The most important observation from XPS measurements is that after etching below the surface layers of the sample (with a surface C/B ratio of 3.8:1), the C/B ratio is maintained between 3.0:1 and 3.3:1. This illustrates that the bulk of the sample of  $C_3B$  is compositionally uniform.

MALDI-TOF mass spectrometry assisted further in characterization and provided further evidence of the homogeneity of the samples. Signals corresponding to  $C_xB_y$  are present in the spectra, with signals associated with  $C_{(x-1)}B_1$  and  $C_{(x-2)}B_2$  being more intense than the corresponding  $C_x$  signals (see Figure S4 in the Supporting Information). The mass spectra, therefore, support the conclusion that B is covalently bound and distributed homogeneously throughout the structure, rather than being present in discrete boron-containing regions. A further important observation is seen from Figure 5, which shows a comparison between the

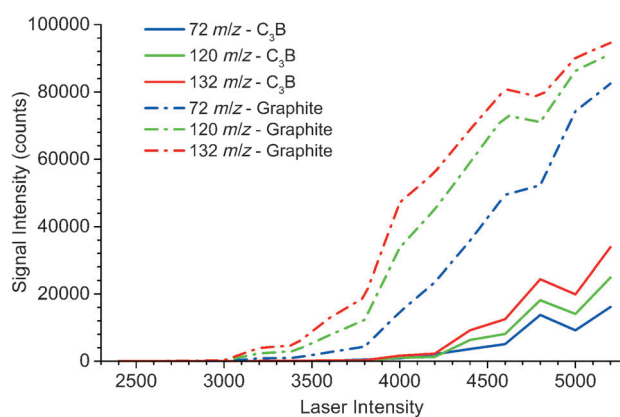


**Figure 5.** Signal intensity as a function of MALDI-TOF MS power, showing how a much greater laser power is required to achieve flight for fragments from  $C_3B$  compared to graphite.

observed signal intensity for a selection of mass fragments with respect to laser power for both a  $C_3B$  and graphite substrate. Despite the chosen mass fragments being based solely on carbon, higher laser powers are required for their generation in  $C_3B$ , which implies incorporation of a heteroatom (in this case boron), which must first be broken away, in the underlying structure.

Solid-state  $^{11}\text{B}$  NMR spectroscopy provides fundamental support for the substitutional incorporation of boron into the structure of  $C_3B$  (shown in Scheme 1, right). First principles calculations of the  $^{11}\text{B}$  NMR parameters (the quadrupolar coupling parameter  $C_Q$  and the anisotropy parameter  $\eta_Q$ ) was performed for boron sites in model  $C_3B$  structures to enable comparison to experimental data. For all structures analyzed, the calculated values remain similar with  $C_Q \approx 5.3 \text{ MHz}$  and  $\eta_Q \approx 0$  (see the Supporting Information for the calculated values and structures). The major component (blue line) in the  $^{11}\text{B}$  echo magic angle spinning (MAS) experiment (Figure 6) at 43 ppm has  $C_Q$  and  $\eta_Q$  values similar to that calculated for  $C_3B$ . The minor components (red lines) are ascribed to boron oxide (see Section S7 in the Supporting Information) impurities. The presence of the dominant

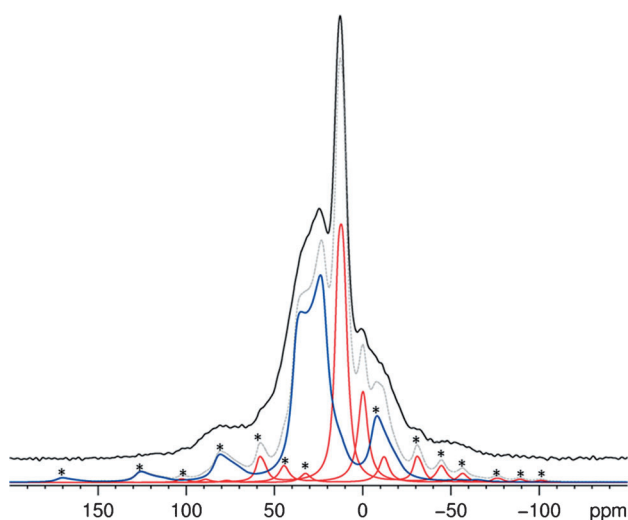


**Figure 6.**  $^{11}\text{B}$  echo ssNMR spectrum acquired at 16.4 T at 10 kHz MAS. The red lines correspond to signals seen in the MQMAS experiment. The blue line was fitted to account for the additional intensity in the spectrum and is assigned to  $\text{C}_3\text{B}$  based on its calculated quadrupolar parameters (further details are given in the Supporting Information). Spinning side bands are marked with an asterisk.

resonance at 43 ppm suggests that boron is present in a substitutional manner in the graphitic lattice.

With well-characterized bulk samples of  $\text{C}_3\text{B}$  in hand, we were next able to assess its  $\text{H}_2$ - and Li-storage characteristics. Hydrogen-storage measurements were performed using a modified Sieverts apparatus. Disappointingly, no significant  $\text{H}_2$  uptake was observed at 77 K or at 295 K between 0 and 20 bar. To test  $\text{C}_3\text{B}$  as a potential lithium ion battery electrode material, coin cells were produced using powdered  $\text{C}_3\text{B}$ . Using a constant current set up, the capacity of the cell was tested over multiple cycles. The capacity achieved during the first charge exceeds  $700 \text{ mA h g}^{-1}$  and on subsequent cycles a reversible capacity of  $374 \text{ mA h g}^{-1}$  was observed (Figure 7). The reversible capacity closely matches that of

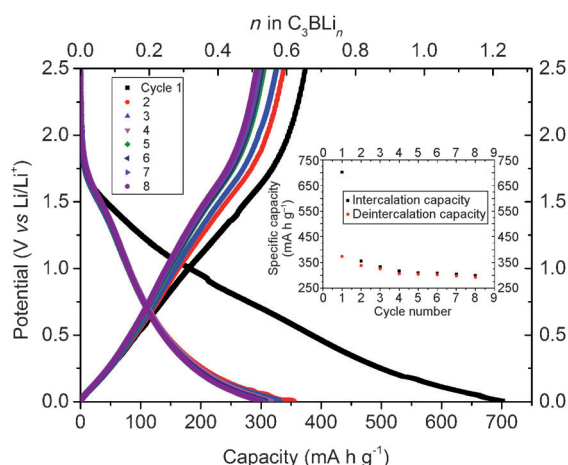


**Figure 7.** Change in potential during the initial discharge and charge cycles. The high capacity seen during the first discharge is irreversible. The insert shows the capacity versus cycle number.

crystalline graphite ( $\text{C}_3\text{BLi}_{0.65}$  cf.  $\text{C}_6\text{Li}$  in graphite). The capacity of the first discharge approaches the theoretical maximum value (corresponding to a formula of  $\text{C}_3\text{BLi}_{1.25}$  versus the maximum of  $\text{C}_3\text{BLi}_{1.5}$ ).<sup>[12]</sup> One possibility is, therefore, that the cell is cycling reversibly between  $\text{C}_3\text{BLi}_{0.65}$  and  $\text{C}_3\text{BLi}_{1.25}$ . Alternatively, however, the irreversible capacity in the first cycle may merely correspond to the formation of a solid-electrolyte interphase layer (SEI).

In conclusion we have reported the first bulk synthesis of the heavily doped graphite  $\text{C}_3\text{B}$ . This has been fully characterized, both compositionally and structurally, as a turbostratic graphitic phase in which boron has substitutionally replaced carbon. With the production of bulk samples we have been able, for the first time, to test previous theoretical predictions of the materials properties of  $\text{C}_3\text{B}$ . Contrary to theory, we find that negligible  $\text{H}_2$  storage occurs. This, and the lower than expected operational Li-storage capacity in a battery, can be traced to a combination of the disorder of the real structure and potentially the adsorption kinetics associated with uptake in micrometer-sized particles. In regard to  $\text{H}_2$  adsorption (see Scheme 2) for example, adjacent boron atoms in a perfect AB stacked structure are required for  $\text{H}_2$  activation. In addition, the maximum theoretical capacity for lithium intercalation into  $\text{C}_3\text{B}$  requires both a highly ordered AB stacking and an ability to convert into the AA stack. The real material instead has been shown to contain randomly orientated layers. Our study suggests that to model the properties of graphitic materials more realistically, the possibility of disorder in particular must be considered.

**Keywords:** boron · graphite ·  $\text{H}_2$  storage · Li battery · synthetic methods

- [1] M. Armand, J.-M. Tarascon, *Nature* **2008**, *451*, 652–657.
- [2] D. J. Durbin, C. Malardier-Jugroot, *Int. J. Hydrogen Energy* **2013**, *38*, 14595–14617.
- [3] R. van Noorden, *Nature* **2014**, *507*, 26.
- [4] P. P. Edwards, V. L. Kuznetsov, W. I. F. David, *Philos. Trans. R. Soc. London Ser. A* **2007**, *365*, 1043–1056.
- [5] M. R. Palacín, *Chem. Soc. Rev.* **2009**, *38*, 2565–2575.
- [6] J. Kouvetakis, R. Kaner, M. Sattler, N. Bartlett, *Chem. Commun.* **1986**, 1758–1759.
- [7] Y.-S. Lee, M. Kertesz, *Chem. Commun.* **1988**, 75.
- [8] C. Zhang, A. Alavi, *J. Chem. Phys.* **2007**, *127*, 214704.
- [9] X. Sha, A. Cooper, W. B. Bailey III, H. Cheng, *J. Phys. Chem. C* **2010**, *114*, 3260–3264.
- [10] US Department of Energy, *US Dep. Energy* **2009**, Revision 4, 1–22.
- [11] B. M. Way, J. R. Dahn, *J. Electrochem. Soc.* **1994**, *141*, 907–912.
- [12] Y. Liu, V. I. Artyukhov, M. Liu, A. R. Harutyunyan, B. I. Yakobson, *J. Phys. Chem. Lett.* **2013**, *4*, 1737–1742.
- [13] J. Kouvetakis, M. McElfresh, D. Beach, *Carbon* **1994**, *32*, 1129–1132.
- [14] T. Shirasaki, A. Tressaud, *Carbon* **2000**, *38*, 1461–1467.
- [15] Z. Jin, Z. Sun, L. J. Simpson, K. J. O'Neill, P. Parilla, Y. Li, N. P. Stadie, C. C. Ahn, C. Kittrell, J. M. Tour, *J. Am. Chem. Soc.* **2010**, *132*, 15246–15251.
- [16] C. Lowell, *J. Am. Ceram. Soc.* **1967**, *50*, 142–144.

- [17] M. C. Haberecht, J. B. Heilmann, A. Haghiri, M. Bolte, J. W. Bats, H.-W. Lerner, M. C. Holthausen, M. Wagner, *Z. Anorg. Allg. Chem.* **2004**, *630*, 904–913.
- [18] T. C. King, P. D. Matthews, J. P. Holgado, D. A. Jefferson, R. M. Lambert, A. Alavi, D. S. Wright, *Carbon* **2013**, *64*, 6–10.
- [19] H. Sun, F. Ribeiro, J.-L. Li, D. Roundy, M. Cohen, S. Louie, *Phys. Rev. B* **2004**, *69*, 024110.
- [20] D. Tomanek, R. Wentzcovitch, S. Louie, M. Cohen, *Phys. Rev. B* **1988**, *37*, 3134–3136.
- [21] This was confirmed by XPS control experiments in which commercial (Aldrich) graphite was analyzed and similar levels of oxygen were observed.

Received: December 19, 2014

Revised: February 18, 2015

Published online: ■ ■ ■ ■, ■ ■ ■ ■

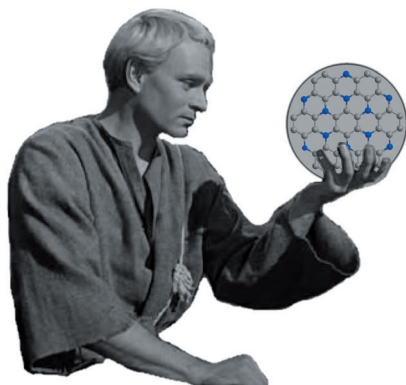
## Communications



### Boron-Doped Graphite

T. C. King, P. D. Matthews, H. Glass,  
J. A. Cormack, J. P. Holgado, M. Leskes,  
J. M. Griffin, O. A. Scherman,  
P. D. Barker, C. P. Grey, S. E. Dutton,  
R. M. Lambert, G. Tustin, A. Alavi,\*  
D. S. Wright\* ————— ■■■■-■■■■

Theory and Practice: Bulk Synthesis of  
 $C_3B$  and its  $H_2$ - and Li-Storage Capacity



**$C_3B$  or not  $C_3B$  that is the question—**  
Previous theoretical predictions suggest that the stoichiometrically doped graphite  $C_3B$  should be a promising  $H_2$ - and Li-storage material, with potentially important applications in power storage. The first experimental measurements of the real material indicate, however, that disorder is a limiting factor for the use of  $C_3B$  as an energy storage material.